EFFECTS OF GRAPHENE SHEET SIZE ON ELECTRICAL CONDUCTIVITY AND PERCOLATION OF GRAPHENE AEROGEL/EPOXY COMPOSITES

Ne Myo Han[1], Zhenyu Wang[1], Xi Shen[1], Ying Wu[1], Xu Liu[1], Qingbin Zheng[1] and Jang-Kyo Kim[1]

[1] Department of Mechanical and Aerospace Engineering, The Hong Kong University of Science and Technology, Clear Water Bay, Kowloon, Hong Kong

Keywords: Graphene aerogel, Sheet size, Electrical conductivity, Percolation, Fracture toughness

ABSTRACT

By varying the size of precursor graphene oxide (GO) sheets, unidirectional graphene aerogels (UGAs) with a wide range of density, alignment and electrical conductivity are prepared. UGAs prepared using ultralarge graphene oxide (UL-UGA) exhibit a low density, a high degree of alignment and a high electrical conductivity. Solid epoxy composites prepared by infiltrating liquid epoxy resin into the UL-UGA structure exhibit an ultralow percolation threshold of 0.0066 vol.%, and a unique anisotropic electrical conductivity. In addition to its electrical conductivity, UL-UGA is shown to be an effective toughening filler, capable of increasing the fracture toughness of epoxy by 69% at 0.11 vol.% graphene content.

1 INTRODUCTION

Electrically conductive fillers, such as metal wires, carbon black (CB), carbon nanotubes (CNTs) and graphene, are added into insulating polymer matrices to produce conductive polymer composites [1]. Graphene aerogel (GA) has recently attracted much attention as an ideal conducting filler due to its ability to retain a 3D interconnected network of conductive graphene sheets within the polymer [2]. Meanwhile, ultralarge graphene oxide (UL-GO) has been shown to produce materials with higher tensile moduli, electrical conductivities and moisture barrier properties than its smaller counterparts [3-6]. The gelation of GO sheets, a critical phenomenon in the formation of aerogel, also depended greatly on their size [7], while the minimum density of graphene aerogels were inversely proportional to their size [8]. Therefore, an ideal strategy to produce ultralight graphene aerogels is by using large graphene sheets. Consequently, producing ultralight graphene aerogels enables the production of a polymer nanocomposite with an ultralow percolation threshold due to the intrinsic 3-D interconnected conductive graphene sheets in the polymer matrix. By fabricating unidirectional graphene aerogels (UGAs) using precursor GO sheets of different sizes, the current study aims to investigate the effects of graphene sheet size on electrical conductivity, percolation threshold and fracture resistance of UGA/epoxy composites.

2 EXPERIMENTAL SECTION

Graphene oxide (GO) was produced from natural graphite flakes (Asbury Graphite Mills) using the modified Hummers method [9], and sorted into three size groups through two-step centrifugation. The procedure for preparing UGA and UGA/epoxy composites is schematically shown in Figure 1. In brief, the GO dispersion was first frozen in a polypropylene (PP) tube using liquid nitrogen, which was then freeze-dried for 48 h to form graphene aerogel (GA). The GA was thermally annealed in air at 200 ^{o}C for 2 h and reduced at 900 ^{o}C in a N_2 atmosphere for 2 h to produce conductive UGAs [3]. Epoxy resin and curing agent were mixed at a weight ratio of 100:12, and was infiltrated into the UGA under vacuum for 2 h. The composite mixture was cured at 80 ^{o}C for 30 min and post-cured at 110 ^{o}C for 2 h to produce solid UGA/epoxy composites.

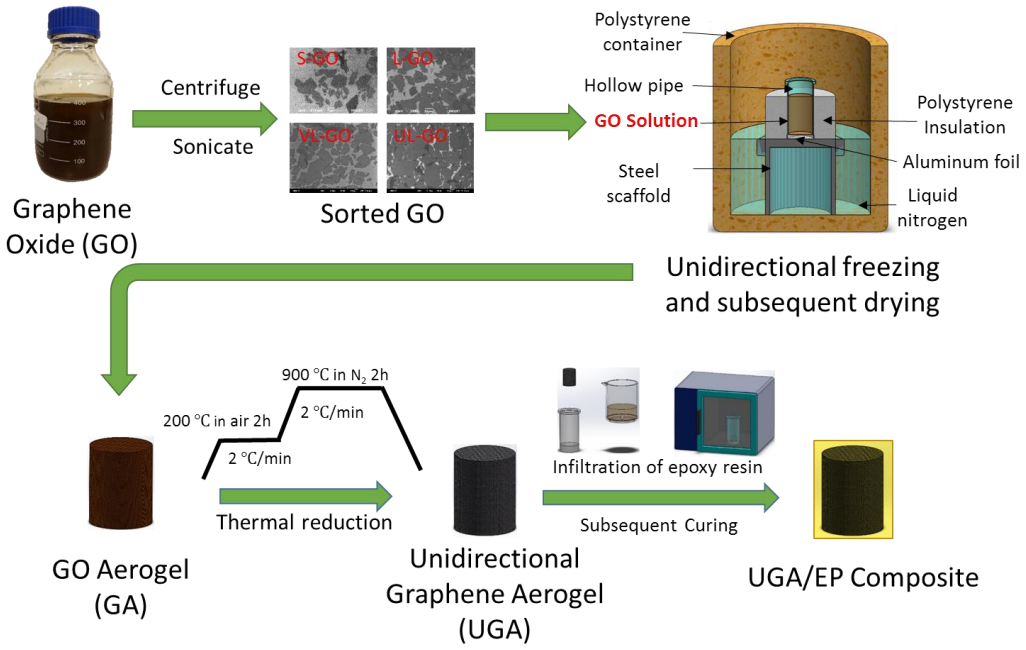

Figure 1: Schematic of the preparation of UGA and UGA/epoxy using GO sheets of different sizes.

Scanning electron microscopy (SEM, JEOL 6390F) was used to characterize GO size, UGA alignment and UGA/epoxy fracture surface. X-ray photoelectron spectroscopy (XPS, Axis Ultra DLD) was used to study elemental compositions of GA and UGA. Raman spectroscopy (Reinshaw MicroRaman) was used to characterize the D- and G- bands of GO and UGA, using He-Ne laser (632.8 nm) at 10% (2.5 mW) power. The universal testing machine (MTS Alliance RT/05) was used to measure the fracture toughness of UGA/epoxy composites using 28 X 6 X 3 mm edge-notched bending samples with a 3 mm pre-crack according to the specification, ASTM D5045 [10].

3 RESULTS AND DISCUSSION

The two-step centrifugation of GO produced sorted GO solutions with average areas of 1.1, 838.0, and 1595.8 μm^2 for small GO (S-GO), large GO (L-GO), and ultralarge GO (UL-GO), respectively. The difference in sheet size between S-GO and UL-GO can be clearly seen in Figure 2.

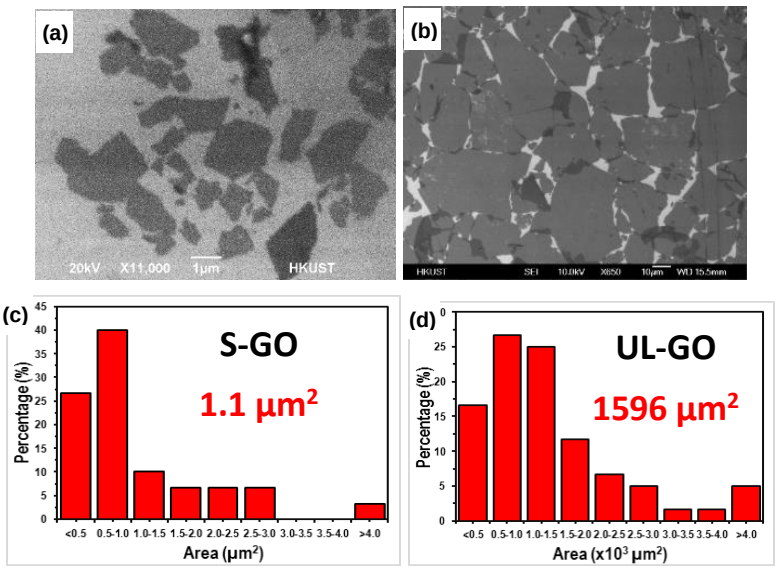

Figure 2: (a, b) SEM images and (c, d) GO size distribution of sorted S-GO and UL-GO sheets.

The UGAs shows a porous structure with 3D interconnected and aligned GO sheets: they exhibit increasing wall thickness and alignment with increasing GO concentration. The UGAs prepared using UL-GO sheets had a higher degree of alignment than those of the S-GO counterpart of the same GO concentration, as shown in Figures 3 (a, b). The degree of alignment is quantified by image analysis and characterized by the orientation factor, $\langle\cos^2\theta_1\rangle$ [12], as shown in Figures 3 (c, d). A fully aligned structure has a $\langle\cos^2\theta_1\rangle$ value of 1, while a fully random 3D structure has a $\langle\cos^2\theta_1\rangle$ value of 0.3. These trends are attributed to the better self-alignment of GO sheets with a higher aspect ratio and concentration. The interlayer spacing between the GO sheets for UGAs produced with 1.0 mg/ml UL-GO was approximately 30 µm.

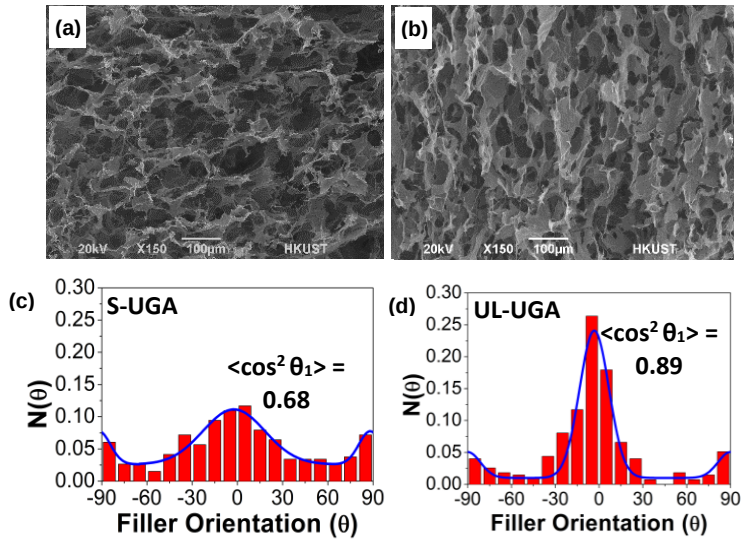

Figure 3: (a, b) SEM images and (c, d) filler orientation factor, $\langle\cos^2\theta_1\rangle$, of S-UGA and UL-UGA.

The XPS deconvoluted C 1s spectra of UL-GO sheets were characterized by the abundant chemical functional groups, such as –C-OH (286.9 eV) and C-C (284.8), with residual peaks of –COOH (289.0 eV), -C=O (287.7 eV) and C-H (285.3 eV), as shown in Figure 4a. The UL-UGA spectra showed a drastic change and elimination of oxygen containing peaks, suggesting that the reduction process effectively removed the oxygenated functional groups from the aerogel. Consequently, the C/O ratio of S-GO and UL-GO aerogels increased from 2.59 to 52.4 and 2.64 to 53.9, respectively. In addition, the Raman spectra given in Figure 4b present a reduction in intensity ratio, I_D/I_G, from 2.36 to 1.51, and downshifts of both the D- and G-band peaks after reduction of UL-GA. These modifications suggest the recovery of sp2 graphitic structure due to the removal of functional groups [11]. These findings prove that the thermal reduction process was effective in reducing GO, giving rise to an enhanced electrical conductivity and mechanical properties of the aerogel and the resulting composites.

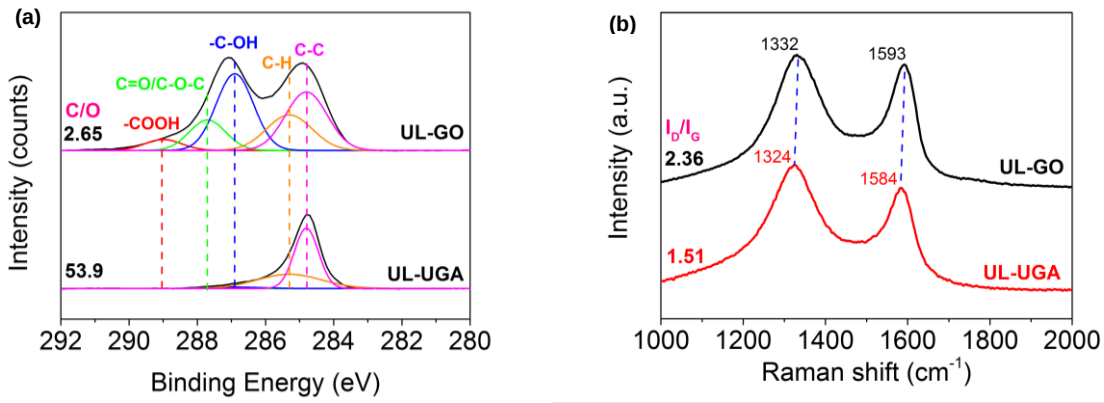

Figure 4: (a) XPS deconvoluted C 1s spectra and (b) Raman spectra of UL-GOA and UL-UGA.

The electrical conductivity of UGA/epoxy composites consistently increased with increasing filler content and GO size, as shown in figure 5a. The UGA fabricated using 2.0 mg/ml of UL-GO sheets exhibited an electrical conductivity of 0.178 S cm^{-1}, while the corresponding UGA/epoxy composite had an electrical conductivity of 0.135 S cm^{-1}. The percolation phenomena were clearly observed for all composites as the conductivity surged from ~10^{-10} to ~10^{-5} S cm^{-1} while the percolation thresholds were different depending on the precursor GO size. The percolation thresholds of the UGA/epoxy composites made from S-GO, L-GO and UL-GO sheets determined using the power law equation were 0.154, 0.033 and 0.0066 vol.%, respectively. The large difference in percolation threshold is expected because the larger GO sheets have an intrinsic ability to form an interconnected 3D network at a lower filler content due to their high aspect ratios than the smaller GO sheets. The comparison of percolation thresholds of representative nanocarbon/polymer nanocomposites is shown in Table 1, clearly indicating the inherently interconnected, highly-aligned current UL-UGA gave rise to a percolation threshold among the lowest nanocarbon composites reported in the literature.

To validate the above finding, a parametric study has been carried out using a method described previously [12] to predict the percolation threshold. The theoretical percolation was calculated using the aspect ratio (D/t), filler orientation as characterized by $\langle\cos^2\theta_1\rangle$ and filler content ratio (V_1/V_2) as the controlling parameters. The percolation factor R is related to these parameters by Equation 1 with the interparticle distance, D_{IP}, assumed to be 10 nm, and translated into the theoretical percolation (V_c) by Equation 2. Because UL-GO had a very high aspect ratio of 41000 capable of producing a highly aligned UGA structure, it possessed high D/t, $\langle\cos^2\theta_1\rangle$ and V_1/V_2 values, giving rise to a high percolation factor and a low theoretical percolation. The model resulted in a theoretical percolation of 0.0033 vol.% for UL-GO and 0.302 vol.% for S-GO UGA, which are in close agreement with the experimental results. A comparison between the experimental results and the theoretical percolation is shown in Figure 5b.

$$R = \frac{(D + D_{IP})^3}{D^2 t} \cdot \frac{\frac{V_1}{V_2} \cdot \langle cos^2\theta_1 \rangle^3 + \langle cos^2\theta_2 \rangle^3}{1 + \frac{V_1}{V_2}} \tag{1}$$

$$V_c = \frac{\pi}{4}\left(\frac{1}{R}\right) \tag{2}$$

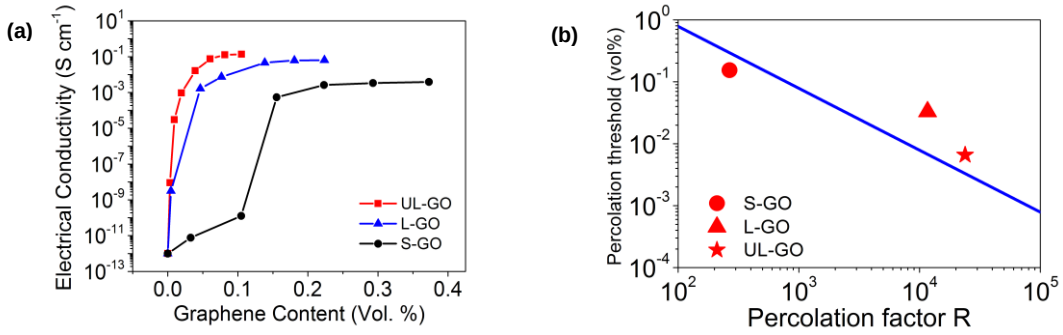

Figure 5: (a) Electrical conductivities measured along the alignment direction as a function of filler content and (b) percolation threshold of UGA/epoxy composites with different GO sizes.

Table 1: Comparison of percolation thresholds of nanocarbon/polymer nanocomposites.

Filler	Polymer Matrix	Processing method	Aspect ratio of filler	Percolation threshold (vol.%)	Reference
CB	PE	Shear mixing	~1	~10	[13]

MWCNT	Epoxy	Sonication	500	0.06	[14]
CB/MWCNT	Epoxy	Shear mixing	CB: ~1 CNT: 670	0.009 (CB), 0.01 (CNT)	[15]
rGO	Epoxy	In situ polymerization	~15000	0.12	[16]
GF	Epoxy	CVD, vacuum infiltration	-	0.028	[17]
UL-UGA	Epoxy	Unidirectional freezing, vac. infiltration	~41000	0.0066	Current study

The fracture toughness of UGA/epoxy was measured in the direction parallel to GO sheets using the single-edge notched bending test. It increased with increasing filler content up to 1.68 MPa $m^{1/2}$ at 0.11 vol.% of UL-GO aerogel, which is 69% higher than that of neat epoxy, as shown in Figure 6 (d). The SEM images of fracture surface, given in Figure 6b, suggest the significant increase in fracture toughness is attributed to crack deflection by the large UL-GO sheets running perpendicular to the crack propagation direction. Extensive debonding at the graphene/epoxy interface is also observed, suggesting the absence of functional groups on the graphene surface, which contributed to fracture toughness enhancement. However, at higher filler contents of 0.16 and 0.22 vol.%, the fracture toughness was rather saturated, possibly a reflection of agglomeration of UGA produced using high GO concentrations, see Figure 6c. This may lead to slippage between the adjacent graphene layers as the dominant failure mode [17]. In contrast, the S-GO UGA was less effective in enhancing the fracture toughness of the composite, with a toughness of up to 1.32 MPa $m^{1/2}$ at 0.16 vol.% due to the limited crack tip deflection.

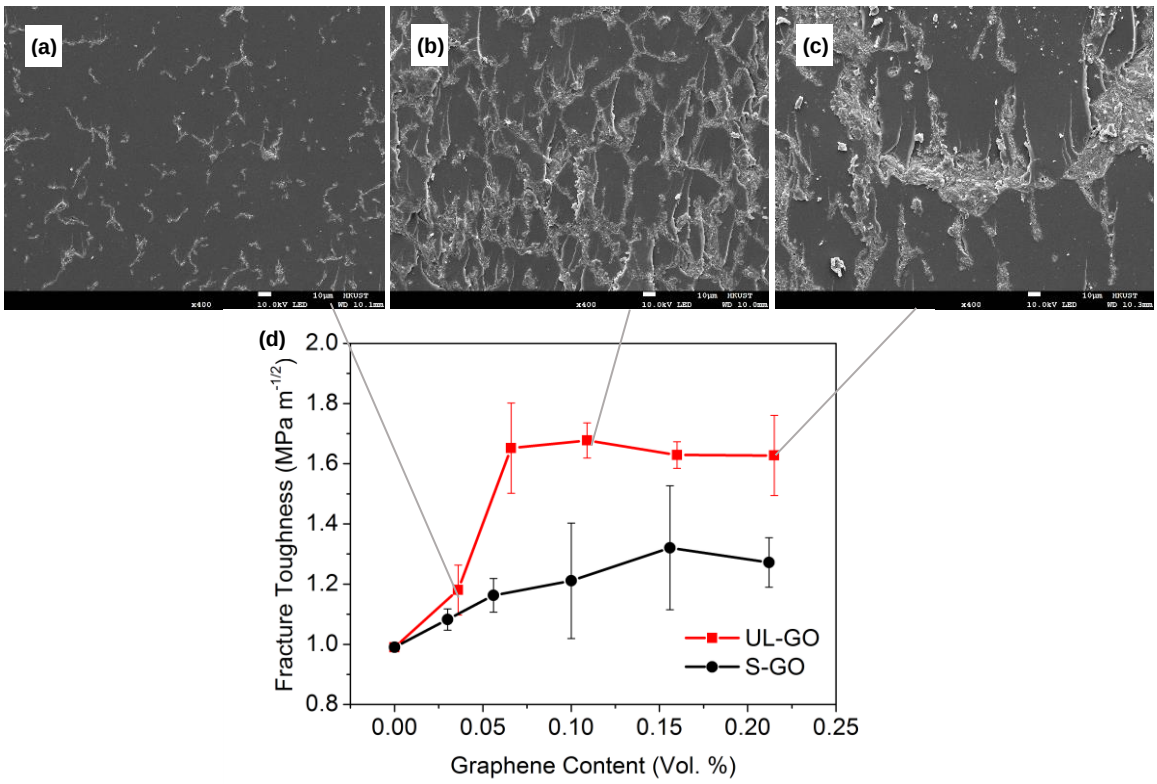

Figure 6: Fracture surface of UGA/epoxy composites made from 0.04 (a), 0.11 (b), and 0.22 (c) vol.% of UL-GO sheets; (d) Fracture toughness UGA/epoxy composites as a function of filler content of different GO sizes.

The comparison of fracture toughness of epoxy nanocomposites containing different types of graphene and CNTs as shown in Figure 7 clearly indicates that 3D interconnected structures were more effective in improving the toughness. The increase in fracture toughness by UL-UGA fillers were comparable to that by CVD-produced graphene foam with a maximum enhancement by around 60-70%. The chemically assembled graphene aerogels fell slightly behind with an increase of 50-60%, while the thermally-reduced GO and multi-walled CNTs dispersed in the matrix were much less effective.

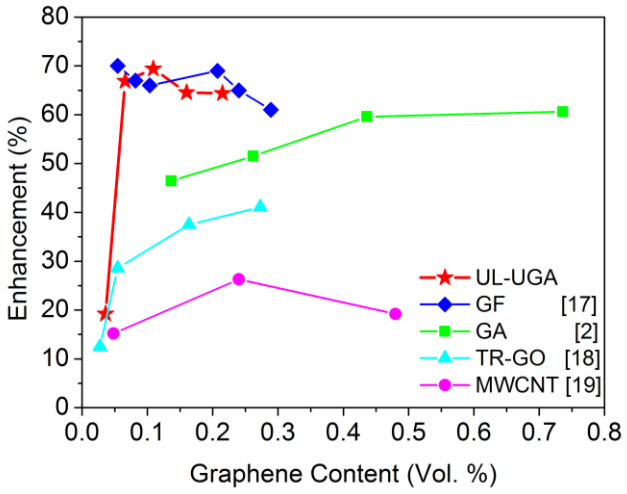

Figure 7: Comparison of fracture toughness enhancements for different nanocarbon/epoxy nanocomposites.

4 CONCLUSION

The effect of GO sheet size on electrical and fracture properties of UGAs and UGA/epoxy composites was studied. Unidirectional freeze casting was employed followed by thermal reduction to fabricate UGAs, which were subsequently infiltrated with epoxy under vacuum to produce UGA/epoxy composite. The electrical conductivities were as high as 0.178 and 0.135 S cm^{-1}, respectively, for the UGA and UGA/EP composite. The S-GO UGA/epoxy composite had a percolation threshold of 0.154 vol.%, while the UL-GO counterpart displayed an ultralow percolation threshold of 0.0066 vol.% due to its high aspect ratio and sheet alignment, which is among the lowest for nanocarbon polymer composites reported in the literature. The experimental percolation thresholds were in good agreement with theory based on an interparticle distance model. The fracture toughness of UGA/epoxy composites were as high as 1.32 MPa $m^{1/2}$ at 0.16 vol.% of S-GO aerogel, and 1.68 MPa $m^{1/2}$ at 0.11 vol.% of UL-GO aerogel. The remarkable 69% increase in fracture toughness compared to neat epoxy for the composites made from UL-UGA is attributed to extensive crack deflection and interfacial debonding. The 3D interconnected, highly aligned and well-reduced UGA structure was responsible for both the excellent electrical conductivity and fracture toughness of the composites.

ACKNOWLEDGEMENTS

The project was supported by the Research Grants Council (GRF Projects: 16203415 and 16229216) of Hong Kong SAR. N.M.H. was a recipient of the Bai Xian Asian Future Leaders Scholarship, while Z.W. and X.S. were recipients of the Hong Kong Ph.D. Fellowship. Technical assistance from Materials Characterization and Preparation Facilities (MCPF), Advanced Engineering Materials Facilities (AEMF), Department of Chemical and Biomolecular Engineering, and Division of Biomedical Engineering at HKUST is appreciated.

REFERENCES

[1] X. Sun, X. Liu, X. Shen, Y. Wu, Z. Wang and J. K. Kim, Graphene foam/carbon nanotube/poly (dimethyl siloxane) composites for exceptional microwave shielding, *Composites Part A: Applied Science and Manufacturing,* **85**, 2016, pp. 199-206.

[2] Z. Wang, X. Shen, M. Akbari Garakani, X. Lin, Y. Wu, X. Liu, X. Sun and J. K. Kim, Graphene aerogel/epoxy composites with exceptional anisotropic structure and properties, *ACS Applied Materials & Interfaces,* **7**, 2015, pp. 5538-5549.

[3] X. Lin, X. Shen, Q. B. Zheng, N. Yousefi, L. Ye, Y. W. Mai and J. K. Kim, Fabrication of highly-aligned, conductive, and strong graphene papers using ultralarge graphene oxide sheets, *ACS Nano,* **6**, 2012, pp. 10708-10719.

[4] N. Yousefi, M. M. Gudarzi, Q. B. Zheng, X. Lin, X. Shen, J. Jia, F. Sharif and J. K. Kim, Highly aligned, ultralarge-size reduced graphene oxide/polyurethane nanocomposites: Mechanical properties and moisture permeability, *Composites Part A: Applied Science and Manufacturing,* **49**, 2013, pp. 42-50.

[5] N. Yousefi, M. M. Gudarzi, Q. Zheng, S. H. Aboutalebi, F. Sharif and J. K. Kim, Self-alignment and high electrical conductivity of ultralarge graphene oxide–polyurethane nanocomposites, *Journal of Materials Chemistry,* **22**, 2012, pp. 12709-12717.

[6] Q. B. Zheng, W. H. Ip, X. Lin, N. Yousefi, K. K. Yeung, Z. Li and J. K. Kim, Transparent conductive films consisting of ultralarge graphene sheets produced by Langmuir–Blodgett assembly, *ACS Nano,* **5**, 2011, pp. 6039-6051.

[7] H. Bai, C. Li, X. Wang and G. Shi, On the gelation of graphene oxide, *The Journal of Physical Chemistry C,* **115**, 2011, pp. 5545-5551.

[8] H. Sun, Z. Xu and C. Gao, Multifunctional, ultra-flyweight, synergistically assembled carbon aerogels, *Advanced Materials,* **25**, 2013, pp. 2554-2560.

[9] S. H. Aboutalebi, M. M. Gudarzi, Q. B. Zheng and J. K. Kim, Spontaneous formation of liquid crystals in ultralarge graphene oxide dispersions, *Advanced Functional Materials,* **21**, 2011, pp. 2978-2988.

[10] B. C. Kim and S. W. Park, Fracture toughness of the nano-particle reinforced epoxy composite, *Composite Structures,* **86**, 2008, pp. 69-77.

[11] A. A. King, B. R. Davies, N. Noorbehesht, P. Newman, T. L. Church, A. T. Harris, J. M. Razal and A. I. Minett, A new raman metric for the characterisation of graphene oxide and its derivatives, *Scientific Reports,* **6**, 2016, pp. 19491.

[12] Z. Wang, X. Shen, N. M. Han, X. Liu, Y. Wu, W. Ye and J. K. Kim, Ultralow electrical percolation in graphene aerogel/epoxy composites, *Chemistry of Materials,* **28**, 2016, pp. 6731-6741.

[13] M. Hindermann-Bischoff and F. Ehrburger-Dolle, Electrical conductivity of carbon black–polyethylene composites: Experimental evidence of the change of cluster connectivity in the PTC effect, *Carbon,* **39**, 2001, pp. 375-382.

[14] J. Li, P. C. Ma, W. S. Chow, C. K. To, B. Z. Tang and J. K. Kim, Correlations between percolation threshold, dispersion state, and aspect ratio of carbon nanotubes, *Advanced Functional Materials*, **17**, 2007, pp. 3207-3215.

[15] J. Sumfleth, X. C. Adroher and K. Schulte, Synergistic effects in network formation and electrical properties of hybrid epoxy nanocomposites containing multi-wall carbon nanotubes and carbon black, *Journal of Materials Science*, **44**, 2009, pp. 3241.

[16] N. Yousefi, X. Lin, Q. Zheng, X. Shen, J. R. Pothnis, J. Jia, E. Zussman and J. K. Kim, Simultaneous in situ reduction, self-alignment and covalent bonding in graphene oxide/epoxy composites, *Carbon*, **59**, 2013, pp. 406-417.

[17] J. Jia, X. Sun, X. Lin, X. Shen, Y. W. Mai and J. K. Kim, Exceptional electrical conductivity and fracture resistance of 3D interconnected graphene foam/epoxy composites, *ACS Nano*, **8**, 2014, pp. 5774-5783.

[18] S. Chandrasekaran, N. Sato, F. Tölle, R. Mülhaupt, B. Fiedler and K. Schulte, Fracture toughness and failure mechanism of graphene based epoxy composites, *Composites Science and Technology*, **97**, 2014, pp. 90-99.

[19] M. Ayatollahi, S. Shadlou and M. Shokrieh, Fracture toughness of epoxy/multi-walled carbon nanotube nano-composites under bending and shear loading conditions, *Materials & Design*, **32**, 2011, pp. 2115-2124.